SHORT COMMUNICATION

Hynd Remita · Prem Felix Siril
Israel-Martyr Mbomekalle · Bineta Keita
Louis Nadjo

Activity evaluation of carbon paste electrodes loaded with pt nanoparticles prepared in different radiolytic conditions

Abstract Three Pt-based catalysts prepared in different radiolytic conditions and supported on graphite powder were packed into a carbon paste electrode configuration. They were compared to each other, to the commercial (Pt) deposited on activated carbon powder (Johnson Matthey) and to pure Vulcan XC-72 for their respective abilities toward the hydrogen evolution reaction (HER). The Tafel parameters were determined for all these electrodes. From the I–V curves and their quantitative treatment, the following order of activity emerged unambiguously and reads: $(PtCO)_2$ (fcc structure) > $(PtCO)_1$ (Chini cluster) > $(Pt)_{neat}$ > $(Pt)_{JM}$ (Johnson Matthey) ≫ (Vulcan XC-72). As expected, all the Pt-loaded electrodes were more efficient than Vulcan XC-72. The classification appears to be linked with the mean nanoparticle size, and for comparable sizes, with the surface morphology of the materials. The results and the stability of the electrodes suggest that the small particle sizes and the good dispersity on the carbon support were maintained during the HER.

Keywords Platinum nanoparticles · Chini clusters · Carbon paste electrodes · Hydrogen evolution reaction

Introduction

Extremely small noble metal particles, in the nanometre range, are interesting in their own right for studying physical properties due to collective phenomena and environment effects [1]. They are also of invaluable interest in several other fields, including heterogeneous catalysis, surface physics and chemistry [1–11]. Radiolytically prepared platinum nanoparticles are the subject of the present work. Platinum and platinum alloys nanoparticles immobilized on high surface area supports such as carbon powder are recognized as promising electrode materials in low-temperature fuel cells [7]. General agreement is being established that particles with a minimum size in the 1–3 nm range ensure the best catalytic efficiency, where they are already metallic in character [12] and with the loose assumption that the nanoparticles are spherical. Several methods of preparation of appropriate nanoparticles with a view to simultaneous or subsequent immobilisation on a support were described, including sputtering, electrochemical deposition, chemical reduction and radiolytic processes [13–16]. Particularly, radiation-induced reduction of metal ions in solution has been demonstrated to be a powerful method to synthesize metal clusters of markedly small and homogeneous controlled size [16]. Colloidal techniques employ various means to limit the size of the particles: a non-exhaustive list includes reducing agents that might also constitute stabilizers such as a the ''citrate'' technique [17], dispersing agents such as polyvinyl alcohol or polyacrylic acid, ligands such as CO or phosphine [16, 18]. For catalyst loading, several methods were used, including impregnation and electrochemical deposition and their positive and negative aspects were discussed [18–23]. In any case, colloidal techniques are claimed to offer the advantage to maintain a low particle size dependence for platinum loading.

As concerns platinum nanoparticles for use in electrocatalysis, several criteria have progressively emerged to define ideal test systems, including size and shape monodispersity, dispersion on a technologically relevant support like graphite, discreteness of individual particles, structure stability before and after the appropriate catalytic process, the absence of stabilizing agents. In particular, several heavy drawbacks are associated with

H. Remita · P. F. Siril · I.-M. Mbomekalle · B. Keita
L. Nadjo (✉)
Laboratoire de Chimie Physique, UMR 8000, CNRS,
Groupe TEMIC, Université Paris-Sud,
Bâtiment 350, 91405 Orsay Cedex, France
E-mail: louis.nadjo@lcp.u-psud.fr
Tel.: +33-1-69157751
Fax: +33-1-69154328

stabilizers. They might not only have a detrimental effect on the electrocatalytic activity of the particles by derivatizing their surface but also add undesired electrical resistance between particles and the electrode surface. Furthermore, any attempt at their removal might induce serious agglomeration of Pt particles. With these criteria in mind, we found it interesting to examine the electrocatalytic behaviours of Pt nanoparticles obtained by radiolytic process in different conditions [15, 16, 18, 24, 25], and which appeared to have very small and uniform sizes. The physical differences observed on varying preparation conditions [24, 25] might induce different electrocatalytic behaviours.

We now compare, in identical experimental conditions, four electrodes, with the same overall platinum loading, for their efficiency in the proton reduction process. The hydrogen evolution reaction (HER) was selected as a good test process for the determination of electrochemical and catalytic characteristics of a new electrode. The catalysts nanoparticles were prepared in different conditions, supported on graphite powder and packed into a carbon paste electrode (CPE) configuration. The comparison was extended to the plain CPE without any catalyst. The outstanding advantages of CPEs in electroanalysis or in electrocatalysis [26–29], in particular upon their modification by metal particles, were discussed in several papers and made them a suitable choice for the present study.

Experimental

General methods and materials

Pure water was used throughout. It was obtained by passing through a RiOs 8 unit followed by a Millipore-Q Academic purification set. All reagents were of high-purity grade and were used as purchased without further purification. The UV-visible spectra were recorded on a HP 845 spectrophotometer. TEM observations were carried out with a type JEM 100 CX II JEOL microscope. The test solutions were 0.5 M H_2SO_4 (pH = 0.33); 0.2 M Na_2SO_4 + H_2SO_4 (pH = 3) and 0.4 M NaH_2PO_4 + NaOH (pH = 7).

Sample and electrode preparations

The solutions contained 10^{-3} M or 2×10^{-3} M K_2PtCl_4 (Aldrich) in water/2-propanol solvent, carefully degassed and then saturated with CO (Alphagaz, 99,94% purity) at atmospheric pressure. The mixture was protected against Pt photoreduction by wrapping the flasks with aluminium foil. The γ-irradiation was carried out in a panoramic ^{60}Co source, which had a maximum dose rate of 4 kGyh^{-1}. The doses needed for complete reduction were 4 and 5.5 kGy for the 10^{-3} M and 2×10^{-3} M K_2PtCl_4 solutions, respectively.

The appropriate amount of colloid solution to obtain 10% w/w Pt/Vulcan XC-72 catalyst was syringed into a flask containing 300 mg of Vulcan XC-72 (a gift of Cabot), which was previously flushed with pure N_2. The mixture was left under stirring for 12 h. The whole process was conducted in dioxygen-free atmosphere. The platinized carbon powder was filtered off, thoroughly rinsed with Millipore water and dried in an oven at 60°C. In the following, these materials are designated by $(PtCO)_1$ and $(PtCO)_2$, depending on the concentration of K_2PtCl_4 (10^{-3} or 2×10^{-3}, respectively) [18, 25, 30] in the initial solution. The material designated by $(Pt)_{neat}$ was obtained by irradiating Pt^{II} in water/0.2 M 2-propanol solutions to scavenge oxidizing OH. radicals (K_2PtCl_4 concentration was 2×10^{-3} M and the dose was 12 kGy) under pure N_2 atmosphere (no ligand nor other stabilizing agents were used). Finally, $(Pt)_{JM}$ with the appropriate 10% Pt-loading on carbon powder was a Johnson Matthey product purchased from Alfa Aesar. The pure Vulcan XC-72 was submitted to the same steps as all the home prepared materials, but in the absence of Pt nanoparticles.

The carbon pastes were prepared by thoroughly hand-mixing 150 mg of Vulcan XC-72 or Pt-loaded Vulcan XC-72 and 100 μl of mineral oil (Aldrich). A portion of these pastes was packed into the end of a glass tube (4 mm inner diameter) and its inner end was connected to a copper wire. The electrode surface was smoothed on a glossy paper. Freshly prepared electrodes were submitted to a few potential cycling in the test solution, after which they show the stable and reproducible voltammograms described and compared in the following. Such electrodes, protected from dust, remained stable for several months in the laboratory atmosphere. They can also be polished gently if necessary.

Electrochemical experiments

Solutions were thoroughly deaerated with pure argon for at least 30 min and kept under a positive pressure of this gas during the experiments. The electrochemical set-up was an EG& G 273 A driven by a PC with the M270 software. Potentials are quoted against a saturated calomel electrode (SCE). The counter electrode was a platinum gauze of large surface area. All experiments were performed at room temperature.

Results and discussion

Surface morphology and average nanoparticle sizes of the various materials

A TEM observation of the three Pt colloids was performed. Representative micrographs are shown in

Fig. 1. The dispersion and homogeneity are remarkable in Fig. 1a, b. Both large Pt aggregates or flocks made up of smaller ones are absent for (Pt)$_{neat}$. The nanoparticles are roughly spherically shaped and homogeneous in shape. However, mean particle size determinations give the following values: 1.0 to 1.2 nm for (PtCO)$_1$, 1.0 nm or less for (PtCO)$_2$ and 1.5 to 2.5 nm for (Pt)$_{neat}$. The last colloid contains bigger nanoparticles than the other two. For further analysis, it is worth reminding that

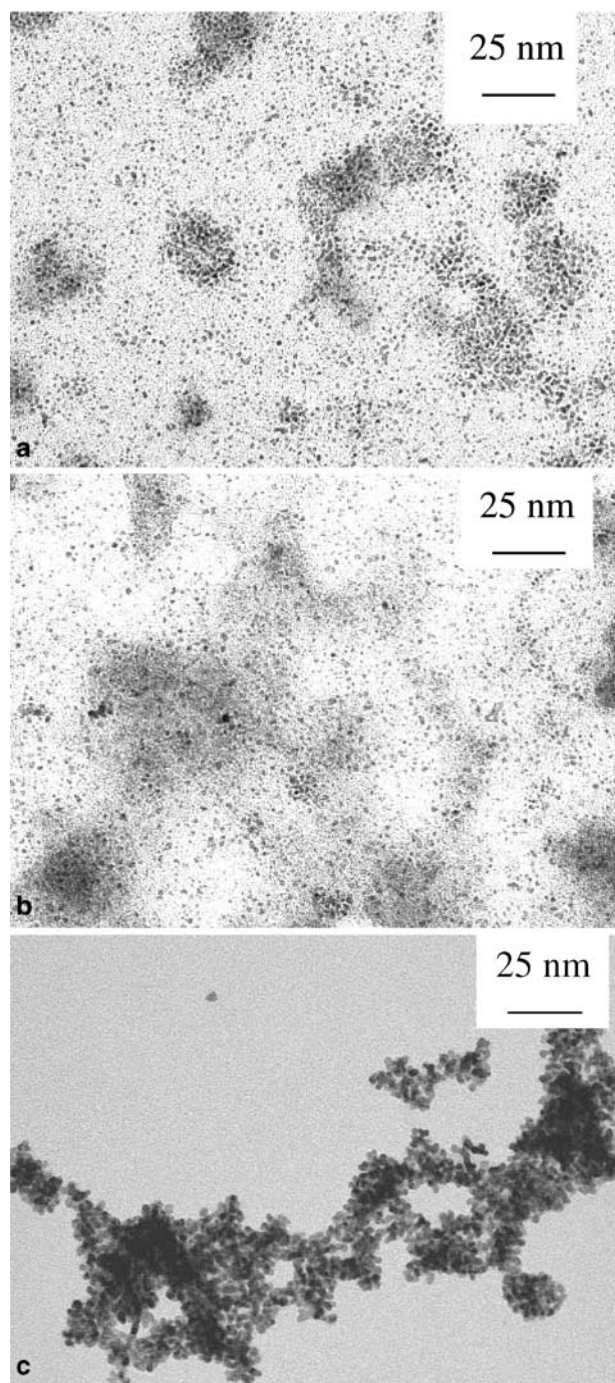**Fig. 1** Micrographs of **a** (PtCO)$_2$ clusters **b** (PtCO)$_1$ Chini clusters and **c** (Pt)γ clusters deposited on carbon grids

(PtCO)$_1$ represents the Chini [Pt$_3$(CO)$_6$]$_n^{2-}$ ($n=6$) clusters which were prepared by irradiating a Pt^{II} complex (at 10^{-3} mole l^{-1}) in an equimolar water/2-propanol solution under CO atmosphere with a gamma ^{60}Co source [30] (dose rate 4 kGy h^{-1}). The optical absorption spectrum of the irradiated solution is identical to the classical spectrum of Chini clusters [30, 31]. Scheme 1 shows the structure of Chini anions [30]. Typically, (PtCO)$_2$ refers to the material prepared by starting from more concentrated solutions of Pt(II) salt, submitted to irradiation under CO atmosphere. It is known [18] that in that case, the typical absorption spectrum of Chini clusters is progressively replaced by the plasmon band of Pt nanoclusters. Moreover, the EXAFS and XRD studies have shown that these samples present fcc Pt crystal structure [25]. Chini molecular clusters become only a minor part.

In a previous work, (PtCO)$_1$ and (PtCO)$_2$ were deposited on different supports, including HOPG and imaged by AFM and STM [30]. In particular, AFM images captured simultaneously in the height mode and the phase-imaging mode, are displayed on a relatively large-scale to highlight the main features of the surface deposit. The difference is striking and illustrates the large sensitivity of the phase lag to variations in material properties.

Typically, the morphology of the (PtCO)$_1$-covered surface is largely dominated by nanowires, which are believed to be formed by a self assembly of elementary linear molecular clusters on the drying step. In addition, STM imaging on HOPG indicated that the structure of initial Chini clusters was transformed into a planar structure keeping the triangular units with the same intra-triangular Pt–Pt distance of 2.66 Å [30]. In contrast, the (PtCO)$_2$-covered surface appears as a patchwork of very numerous domains. Actually, these domains are constituted by nodules and a few fibrils, thus revealing the evolution at increasing concentration during the synthesis from incomplete topmost layers with several
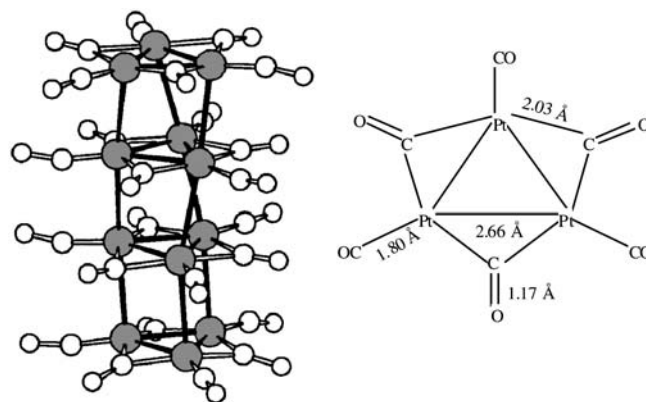

Scheme 1 Structure of Chini dianions [Pt$_3$(CO)$_6$]$_n^{2-}$ clusters ($n=4$). They are formed by a twisted prismatic of n stacking triangular units Pt$_3$(CO)$_6$. The intertriangular Pt–Pt distance between stacked units is 3.08–3.10 Å for $n=3$–6

random islands of clusters toward a dense layer. The qualitative visual difference in morphology between these surfaces is striking. In short, near-field microscopy images indicate an obvious difference in surface structures between $(PtCO)_1$ and $(PtCO)_2$.

Activity of the modified CPEs in the hydrogen evolution reaction (HER) in pH 0.33 sulphate medium

Figure 2 shows, in superposition, the CVs obtained with the different electrodes in pH 0.33 sulphate medium. It appeared clearly, upon simple visual inspection, that the catalytic behaviour for the HER of the Pt-loaded electrodes is better than that of pure Vulcan XC-72. The HER onset is more favourable in the order $(PtCO)_2 > (PtCO)_1 > (Pt)_{neat} > (Pt)_{JM} \gg$ (Vulcan XC-72). For a quantitative characterization of this process, classical Tafel analysis was performed in the high overpotential approximation regime to ensure kinetic control of the HER. Owing to the high proton concentration, mass transport effects on the current were neglected. In these conditions the following Eq. 1 was valid

$$\eta = (RT/\alpha nF)\ln i_0 - (RT/)\ln i. \qquad (1)$$
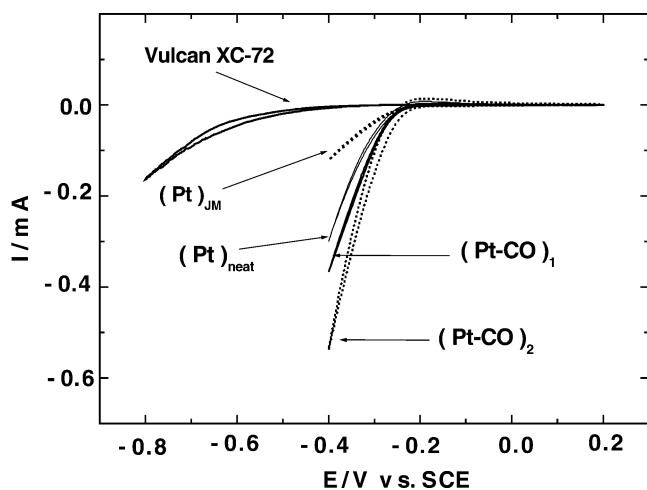
Fig. 2 Cyclic voltammograms run in 0.5 M H_2SO_4 (pH = 0.33) and restricted to the respective HER onset domains for the various Pt-loaded CPE electrodes and for pure Vulcan XC-72. Potential scan rate was 2 mV s^{-1}; the reference electrode was a SCE

The main parameters calculated from the Tafel plots are gathered in Table 1. The indicated Tafel slopes refer to the η vs $\log i$ plots and α is the cathodic transfer coefficientas defined for multistep n-electron transfer processes with possible chemical steps included.

For each electrode, the observed Tafel slopes and the exchange current densities were very close from one scan rate to the other when the latter varied from 10 to 2 mVs^{-1} and the differences remained in the range of experimental fluctuations. This result supports the neglect of mass transfer effects in the present analysis. The values in Table 1 call for several comments. The characteristics of pure Vulcan XC-72 indicated that the catalytic behaviour of this material toward the HER was intermediate between that of freshly polished glassy carbon (GC) for which (-log i_0) was found to vary from 7.2 to 8.5 (with α from 0.15 to 0.28) and that of glassy carbon treated in 0.5 M H_2SO_4 medium for which (-log i_0) was 3.97 (with $\alpha = 0.38$) [32]. In spite of their modest platinum loading, all the other electrodes proved remarkably activated compared to pure Vulcan XC 72. It might be noted that $(Pt)_{JM}$ displayed the highest Tafel slope in the series of electrodes. Except for the cases of pure Vulcan XC-72 and $(Pt)_{JM}$, all the other electrode materials showed similar Tafel parameters, with the Tafel slopes ranging from 0.160 to 0.183 V and the (-log i_0) values from 4.12 to 3.49. Yet, on scrutiny, the order of catalytic activity established qualitatively upon examination of the current-potential curves was confirmed here on the quantitative basis of exchange current densities and reads:

$$(PtCO)_2 > (PtCO)_1 > (Pt)\gamma > (Pt)_{JM}$$
$$\gg (Vulcan\ XC-72).$$

The parameter values in Table 1 are useful as a guide for comparisons among the various electrodes. However, direct comparison with published HER parameter values for bulky platinum will not be made [33]. The reasons include the fact that drastic purity conditions necessary for discussion of mechanistic pathways of the HER on bulky platinum are beyond the scope of the present work; in contrast with the calculations in Table 1, exchange current densities for bulky platinum are always given for real surface area of the platinum electrode, sometimes within the accuracy of roughness factor; finally, the exchange current density value which could have been referred to in reference [33] is obtained by extrapolation of

Table 1 Tafel parameters for the HER on CPEs modified with Pt nanoparticles synthesized in various ways

Electrode geometrical surface area: $S = 0.385$ cm^2. For further details, see text

		Electrode	Carbon Vulcan XC 72	$(Pt)_{JM}$	$(Pt)\gamma$	$(PtCO)_1$	$(PtCO)_2$
$v = 10$ mV s^{-1}		slope (V)	0.127	0.231	0.170	0.170	0.175
		$-\log i_0$	5.99	3.92	3.72	3.64	3.49
		α	0.46	0.26	0.35	0.35	0.34
$v = 2$ mV s^{-1}		slope (V)	0.120	0.208	0.160	0.175	0.183
		$-\log i_0$	6.13	4.13	3.94	3.77	3.58
		α	0.49	0.28	0.37	0.34	0.32

510

Tafel region with low (ca. 30 mV) slope. In short, the aim of the present work is to demonstrate that even very low platinum nanoparticles loading into carbon powder activates substantially the corresponding electrodes but not to discuss and compare the mechanistic pathways of the HER on bulky platinum with Pt-loaded CPE electrodes.

It has been known for a long time that different preparation conditions, including the nature of the metal precursors, lead to different morphological characteristics for catalysts [14]. As a consequence, direct comparison of their electrochemical performances for the same process is a tentative issue, the conclusions of which must be restricted to firmly established experimental evidences. In the present examples, the overall platinum loading is the common basis for such a comparison, but at least, the (PtCO) species are anticipated to generate morphologically different catalysts [18, 30]. The particle sizes ranged from 1.0 to 2.5 nm, with the size for $(Pt)_{neat}$ appearing in the upper side of the domain [14, 29]. The particle size increases generally with the catalyst loading, even though this parameter could be made independent of the catalyst loading and support surface area in impregnation techniques [18]. For $(Pt)_{JM}$ supported on an activated carbon powder with a specific surface area from 900 to 1,100 m^2 g^{-1}, its particle size, measured at 40% Pt loading, ranged from 3.8 to 4.0 nm [23]. Combination of these two characteristics might explain the behaviour of this material as compared to all the other Pt-loaded materials of this work. Among the materials prepared and tested in this work, $(PtCO)_2$ appeared as the most efficient for the HER, followed immediately by $(PtCO)_1$. Even though both materials were CO-stabilized, their difference in electrocatalytic activity toward the HER suggests that morphology variations differentiate between their electrocatalytic abilities for the HER. The foregoing considerations would indicate two important parameters in the HER by Pt nanoparticles—an average particle size between 1.0 and 2.5 nm and the surface morphology of the nano-aggregates.

Any more detailed discussion of the relationship between the particles' morphology and size and their electrocatalytic activity toward the HER is beyond the scope of the present communication.

The same comparisons were performed in pH = 3 and pH = 7 test solutions and showed qualitatively the same classification of the electrode materials. The observation is also interesting in that it indicates that these materials remain efficient in these media.

Pt-CO electrodes were also found to be efficient toward the dioxygen reduction. In a pH = 0.33 solution and at + 0.2 V vs SCE, the current measured on $(PtCO)_2$ is twice as large as that measured on $(Pt)_{JM}$. In these conditions, pure Vulcan XC-72 does not show any activity for this process.

The present electrodes were stable in all the test solutions and could be reused for several months without alteration.

Work in progress will develop such comparisons and other applications in electrocatalysis and electroanalysis.

Conclusion

In this work, three Pt-based catalysts prepared in different conditions and supported on graphite powder were packed into a carbon paste electrode (CPE) configuration. They were compared to each other and to $(Pt)_{JM}$ and pure Vulcan XC-72 for their respective abilities toward the HER. Among all the Pt-loaded electrodes, the three materials prepared in this laboratory came out to be more efficient than the commercial compound $(Pt)_{JM}$. In spite of the closeness of the measured Tafel parameters for these electrodes, an order of activity emerged unambiguously and reads: $(PtCO)_2 > (PtCO)_1 > (Pt)_{neat} > (Pt)_{JM} \gg$ (Vulcan XC-72). This classification appears to be linked essentially with two main parameters: the mean nanoparticle size, and for comparable sizes, the surface morphology of the materials. The results and the stability of the electrodes suggest that the small particle sizes and the good dispersity on the carbon support were maintained during the HER.

References

1. Schmid G (ed) (1994) Clusters and Colloids: From Theory to Applications. Weinheim, New York
2. Henglein A (1993) J Phys Chem 97:5457
3. Lin Y, Finke RG (1994) J Am Chem Soc 116:8335
4. Widegren JA, Aiken JD III, Özcar S, Finke RG (2001) Chem Mater 13:312
5. Özcar S, Finke RG (2002) J Am Chem Soc 124:5796
6. El-Sayed MA (2001) Acc Chem Res 34:257
7. Dillon R, Srinivasan S, Aricò AS, Antonucci V (2003) J Power Sources 127:112
8. Schmidt TJ, Gesteiger HA, Behm R (1999) Electrochem Commun 1:1
9. Leite ER, Wever IT, Longo E, Varela JA (2000) Adv Mater 12:965
10. Zoval JV, Lee J, Gorer S, Penner RM (1998) J Phys Chem B 102:1166
11. Yohannes K (1996) J Electrochem Soc 143:2152
12. Takasu Y, Ohashi N, Zhang XG, Murakami N, Minagawa H, Sato S, Yahikozawa K (1996) Electrochimica Acta 41:2595
13. Goia DV, Matijevic E (1998) New J Chem 1203
14. Lizcano-Valbuena WH, de Azevedo DC, Gonzalez ER (2004) Electrochimica Acta 49:1289
15. Gachard E, Remita H, Khatouri J, Keita B, Nadjo L, Belloni J (1998) New J Chem 1257
16. Belloni J, Mostafavi M, Remita H, Marignier JL, Delcourt MO (1998) New J Chem 1239
17. Aika K, Ban LL, Okura I, Namba S, Turkevich J (1976) J Res Inst Catal 24:54

18. Le Gratiet B, Remita H, Picq G, Delcourt MO (1996) J Catal 164:36
19. Shaikhutdinov SK, Möller FA, Mestl G, Behm RJ (1996) J Catal 163:492
20. Pron'kin SN, Tsirlina GA, Petrii OA, Yu Vassiliev S (2001) Electrochimica Acta 46:2343
21. You T, Niwa O, Tomita M, Hirono S (2003) Anal Chem 75:2080
22. Xu Z, Qi Z, Kaufman A (2003) J Chem Soc Chem Commun 878
23. Zhou Z, Wang S, Zhou W, Wang G, Jiang L, Li W, Song S, Liu J, Sun G, Xin Q (2003) J Chem Soc Chem Commun 394
24. Le Gratiet B, Remita H, Picq G, Delcourt MO (1996) Radiat Phys Chem 47:263
25. Torigoe K, Remita H, Picq G, Belloni J, Bazin D (2000) J Phys Chem B 104:7050
26. Merz A (1990) Top Curr Chem 152:49
27. Murray RW (ed) (1992) Molecular design of electrode surfaces. Wiley, New York
28. Wang J, Naser N, Angnes L, Wu H, Chen L (1992) Anal Chem 64:1285
29. Lubert KH, Guttmann M, Beyer L (1999) J Electroanal Chem 462:174
30. Remita H, Keita B, Torigoe G, Belloni J, Nadjo L (2004) Surf Sci 572:301
31. Treguer M, Remita H, Pernot P, Khatouri J, Belloni J (2001) J Phys Chem A 105:6102
32. Keita B, Nadjo L, Parsons R (1989) J Electroanal Chem 258:207
33. Trasatti S (1972) J Electroanal Chem 39:163